

# Wiskott-Aldrich syndrome iPSC cells produce megakaryocytes with defects in cytoskeletal rearrangement and proplatelet formation

Praewphan Ingrungruanglert<sup>1\*</sup>; Pramuk Amarinthnukrowh<sup>2,3\*</sup>; Ruttachuk Rungsiwuwut<sup>4</sup>; Supang Maneesri-le Grand<sup>5</sup>; Darintr Sosothikul<sup>6</sup>; Kanya Suphapeetiporn<sup>2,3</sup>; Nipan Israsena<sup>1,7</sup>; Vorasuk Shotelersuk<sup>2,3</sup>

<sup>1</sup>Stem Cell and Cell Therapy Research Unit, Faculty of Medicine, Chulalongkorn University, Bangkok, Thailand; <sup>2</sup>Center of Excellence for Medical Genetics, Department of Pediatrics, Faculty of Medicine, Chulalongkorn University, Bangkok, Thailand; <sup>3</sup>Excellence Center for Medical Genetics, King Chulalongkorn Memorial Hospital, Thai Red Cross Society, Bangkok, Thailand; <sup>4</sup>Human Embryonic Stem Cell Research Center, Department of Obstetrics and Gynecology, Faculty of Medicine, Chulalongkorn University, Bangkok, Thailand; <sup>5</sup>Department of Pathology, Faculty of Medicine, Chulalongkorn University, Bangkok, Thailand; <sup>6</sup>Division of Pediatric Hematology/Oncology, Department of Pediatrics, Faculty of Medicine, Chulalongkorn University, Bangkok, Thailand; <sup>7</sup>Department of Pharmacology, Faculty of Medicine, Chulalongkorn University, Bangkok, Thailand

## Summary

Wiskott-Aldrich syndrome (WAS) is an X-linked recessive disorder characterised by microthrombocytopenia, complex immunodeficiency, autoimmunity, and haematologic malignancies. It is caused by mutations in the gene encoding WAS protein (WASP), a regulator of actin cytoskeleton and chromatin structure in various blood cell lineages. The molecular mechanisms underlying microthrombocytopenia caused by WASP mutations remain elusive. Murine models of WASP deficiency exhibited only mild thrombocytopenia with normal-sized platelets. Here we report on the successful generation of induced pluripotent stem cell (iPSC) lines from two patients with different mutations in WASP (c.1507T>A and c.55C>T). When differentiated into early CD34<sup>+</sup> haematopoietic and megakaryocyte progenitors, the WAS-iPSC lines were indistinguishable from the wild-type iPSCs. How-

ever, all WAS-iPSC lines exhibited defects in platelet production *in vitro*. WAS-iPSCs produced platelets with more irregular shapes and smaller sizes. Immunofluorescence and electron micrograph showed defects in cytoskeletal rearrangement, F-actin distribution, and proplatelet formation. Proplatelet defects were more pronounced when using culture systems with stromal feeders comparing to feeder-free culture condition. Overexpression of WASP in the WAS-iPSCs using a lentiviral vector improved proplatelet structures and increased the platelet size. Our findings substantiate the use of iPSC technology to elucidate the disease mechanisms of WAS in thrombopoiesis.

## Keywords

Wiskott-Aldrich syndrome, WASP, iPSCs, platelet, thrombopoiesis

## Correspondence to:

Kanya Suphapeetiporn, MD, PhD  
Head, Division of Medical Genetics and Metabolism  
Sor Kor Building 11th floor  
Department of Pediatrics, Faculty of Medicine  
Chulalongkorn University  
Bangkok 10330, Thailand  
Tel.: +662 256 4951, Fax: +662 256 4000 Ext 3589  
E-mail: kanya.su@chula.ac.th

or

Nipan Israsena, MD, PhD  
Head, Stem Cell and Cell Therapy  
Research Unit, Chulalongkorn University  
Bangkok 10330, Thailand  
Tel.: +662 256 4000 Ext 3589, Fax: +662 256 4911  
E-mail: nipan.i@chula.ac.th

Received: June 11, 2014

Accepted after major revision: November 4, 2014

Epub ahead of print: December 18, 2014

<http://dx.doi.org/10.1160/TH14-06-0503>

Thromb Haemost 2015; 113: ■■■

\* These authors contributed equally to this work.

## Introduction

The discovery of induced pluripotent stem cell (iPSC) technology in 2006 (1) has revolutionised the field of regenerative medicine. It provides potentially unlimited sources for generating disease-relevant cell types for autologous cell therapy and efficient methods for studying disease processes. While transgenic mouse models have been invaluable tools for the study of genetic disorders in humans, studies in mice have significant limitations including biological differences between humans and mice. Recent reports have demonstrated that cells differentiated from iPSCs derived from

patients with genetic diseases (2–4), exhibit abnormal phenotypes *in vitro*. These cellular models have been developed and therefore become new tools for conducting rapid high-throughput drug screening, developing effective gene targeting strategies, and addressing the species-specific features (5, 6).

Wiskott-Aldrich syndrome (WAS; MIM 301000) is an X-linked recessive disorder with a wide spectrum of clinical phenotypes. While the milder form, X-linked thrombocytopenia (XLT; MIM 313900) has thrombocytopenia with absent or minor infections and eczema, the most severe form, classic WAS exhibits microthrombocytopenia, complex immunodeficiency, as well as an in-

creased risk in developing autoimmune disorders and hematologic malignancies (7). Patients with severe WAS mostly die at a young age. WAS is caused by mutations in the gene encoding WAS protein (WASP). The WASP is expressed in all haematopoietic lineages. While its exact functions remain unclear, evidence suggests that it participates in the re-organisation of actin cytoskeleton of haematopoietic and immune cells in response to extra-cellular stimuli (8, 9). In addition, expression of WASP could confer selective advantage for specific haematopoietic cell populations (8). Recently, it has been shown that WASP also acts in the nucleus to regulate epigenetic status of genes involved in T-cell differentiation (10). Gain-of-function mutations in the *WASP* gene produce a distinct clinical phenotype of neutropenia and myelodysplasia in the absence of thrombocytopenia and T-cell immune deficiency (11, 12).

In contrast to human phenotypes, murine models of WASP deficiency exhibited only mild thrombocytopenia with normal-sized platelets (13). In addition, they did not develop eczema, abnormal bleeding or haematopoietic malignancies. The bone marrow of WASP deficient mice showed more megakaryocytes with ectopic and premature proplatelet formation (14) suggesting the possibility of ineffective platelet production as the pathomechanism of thrombocytopenia. However, studies in humans provided mixed results. While some studies showed that mutations in the *WASP* gene resulted in defects of megakaryocyte generation and differentiation (15), others demonstrated that megakaryocytes from WAS patients could mature and form proplatelet normally (16). In addition, the number of megakaryocytes in the bone marrow of WAS patients was usually found to be normal.

A number of protocols for generating haematopoietic progenitors, and most mature haematopoietic cell types have been reported (17–19). In 2008 Takayama et al. developed a method for differentiating pluripotent stem cells into functional platelets (20, 21). Platelets derived from human embryonic stem cells (ESCs) and iPSCs were capable of promoting clot formation when transfused into an animal model (20, 22). Unlike adult haematopoietic stem cells (HSCs), iPSCs can be easily genetically manipulated and clonally expanded; thus provide a new opportunity for studying the role of various genes in platelet biogenesis (23).

In this study, we reported on the generation of patient-specific iPSCs from fibroblasts obtained from two unrelated WAS patients. Using *in vitro* differentiation system, we demonstrated that WAS-iPSCs could produce megakaryocytes and platelets with WAS phenotypes.

## Materials and methods

### Generation of iPSCs

Dermal fibroblasts from two previously reported WAS patients (24, 25) and two unrelated normal individuals were obtained from skin biopsies. Studies using human cells were approved by the institutional review board of the Faculty of Medicine of Chulalongkorn University and were conducted in accordance with the Declaration of Helsinki.

ReV-iPSCs were generated using the following methods. A total of  $6 \times 10^6$  GP-293 cells were transfected with 13  $\mu\text{g}$  of each retroviral vector (Addgene, Cambridge, MA, USA), pMIG-OCT4 (clone 17225), pMIG-SOX2 (clone 17226), pMIG-KLF4 (clone 17227), pMXS-cMYC (clone 13375), and 5  $\mu\text{g}$  of pVSV-G (Clontech, Palo Alto, CA, USA) using X-tremeGENE HP DNA Transfection Reagent (Roche, Indianapolis, IN, USA). At 48 hours (h) after transfection, the media were collected and filtered through a 0.45- $\mu\text{m}$  pore size filter. Virus-containing supernatants were centrifuged at 25,000 rpm for 90 minutes (min). Viral pellets were resuspended with Opti-MEM (Invitrogen, Carlsbad, CA, USA). Human fibroblasts were transduced with the OKSM retrovirus cocktail supplemented with 6  $\mu\text{g}/\text{ml}$  polybrene. Five days after transduction, transduced fibroblasts were seeded onto mitotically inactivated human foreskin fibroblasts and cultured with iPS media until an emerging of iPS colonies.

SeV-iPSCs were generated by using temperature sensitive Sendai virus (SeV) vectors (TS7) encoding Oct3/4, Sox2, Klf4 and c-Myc (a gift from DNAVEC, Japan). The reprogramming procedure was performed as previously described (26–28).

Chula2, a human embryonic stem cell (hESC) line (29), was used as a control.

To generate lentiviral vectors expressing WASP, the WASP coding sequence was cloned into the pLenti6.3/TO/V5-DEST (Invitrogen) using LR Clonase<sup>®</sup> II (Invitrogen). 293FT cells were transfected with 5  $\mu\text{g}$  of each pLenti6.3/TO/WASP, pLP1, pLP2 and pVSV-G (Invitrogen) using X-tremeGENE HP DNA Transfection Reagent (Roche). Two days after transfection, the media were collected and filtered through a 0.45- $\mu\text{m}$  pore size filter. Virus-containing supernatants were centrifuged at 25,000 rpm for 90 min. Viral pellets were resuspended with Opti-MEM (Invitrogen). Haematopoietic progenitor cells from ES-sacs on day 14 were transduced with lentiviruses supplemented with 6  $\mu\text{g}/\text{ml}$  polybrene. At 24 h after transduction, cells were reseeded onto mitotically inactivated OP9 feeder cells and cultured in the megakaryocyte differentiation medium.

### Immunofluorescence staining

Human iPSCs were fixed with 4% formaldehyde for 15 min at room temperature and then permeabilised with 1XPBS supplemented with 0.3% Triton X-100 for 15 min. Human iPSCs were then blocked in blocking solution (10% goat serum and 0.3% Triton X-100 in PBS) for 30 min at room temperature and stained with primary antibodies, Oct4, Nanog, Tra-1-60, Tra-1-181 (StemLite<sup>™</sup> Pluripotency IF kit, Cell Signaling, Danvers, MA, USA) at 4°C overnight. Cells were stained with the Alexa Fluor conjugated secondary antibody (Molecular Probes, Invitrogen) for 1 h. For Sendai virus detection, anti-Sendai virus (PD029, Medical & Biological Laboratories Co., Ltd., Sendai, Japan) was used as a primary antibody.

For platelet staining, platelet-containing supernatant containing 1  $\mu\text{M}$  prostaglandin E1 was centrifuged at 2,000 rpm. Platelet pellet was resuspended and smeared onto the poly-L-lysine coated cover slide and dried. For proplatelet staining, iPSC-derived mega-

karyocytes on day 21 of culture were reseeded onto coverslips coated with matrigel and cultured for 24 h. Then, slides were fixed with 4% formaldehyde for 15 min at room temperature and then permeabilised with 1XPBS supplemented with 0.3% Triton X-100 for 15 min. Proplatelets and platelets were then blocked in the blocking solution for 30 min at room temperature and stained with anti- $\alpha$ -tubulin (Abcam, Cambridge, MA, USA) and phalloidin-FITC (Molecular Probes, Invitrogen). For WASP overexpression experiment, proplatelets were stained with anti-WASP (Abcam) and phalloidin-FITC, and platelets were stained with anti-WASP (Abcam) and anti- $\alpha$ -tubulin (Abcam). For F-actin staining, iPSC-derived megakaryocytes on day 24 of culture were re-plated onto coverslips coated with collagen type I and cultured for 2 h. Then, cells were fixed, permeabilised and blocked. Cells were subsequently stained with anti CD42b-PE (BioLegend, San Diego, CA, USA) and phalloidin-FITC. One  $\mu\text{g}/\text{ml}$  DAPI (Molecular Probes, Invitrogen) was used for nuclear staining. All fluorescence images were obtained by using Axio Observer fluorescence microscope (Carl Zeiss, Jena, Germany). The shortest diameter of tubulin-stained discoid-shaped platelets was measured by using AxioVision Rel 4.8 (Carl Zeiss).

### Reverse transcription-polymerase chain reaction (RT-PCR) and real-time PCR

Total RNA was extracted by using TRI reagent (Molecular Research Center, Cincinnati, OH, USA). Isolated RNA was reverse transcribed with RevertAid™ H Minus M-MuLV (Fermentas, Glen Burnie, MD, USA). Real-time PCR assay was performed by using Maxima SYBR Green/ROX qPCR Master Mix (2X) (Fermentas) on ABI 7500 Fast Real-Time PCR System.

### Western blot for WASP expression

Forty  $\mu\text{g}$  of total protein lysates were mixed with 6X loading dye, Laemmli sample buffer, boiled at 95°C for 5 min, and loaded onto 10% sodium dodecylsulfate polyacrylamide gel. A mouse anti-WASP monoclonal antibody raised against a recombinant protein corresponding to the N-terminal region of human WASP (B-9; Santa Cruz Biotechnology, Santa Cruz, CA, USA) and a goat anti-mouse IgG2a-HRP (sc-2005; Santa Cruz Biotechnology) were used as primary and secondary antibodies, respectively. GAPDH was used as a control for protein loading.

### Colony forming cell (CFC) assay

All haematopoietic progenitor assays were performed according to the manufacturer's instructions (STEMCELL Technologies, Vancouver, BC, Canada). Briefly, 16,500 progenitor cells were added to 3.3 ml of methylcellulose media (MethoCult™ H4034 Optimum) and mixed. Then, 1 ml of methylcellulose media containing cells was plated onto a 35-mm petri dish in duplicate using a 3-ml syringe attached to a 16 gauge blunt-end needle. Methylcellulose cultures were incubated for 12 to 14 days at 37°C in a humidified incubator with 5% CO<sub>2</sub>. The total number of colonies per dish was

scored on day 12 to 14. Human megakaryocyte progenitors were analysed using MegaCult®-C (STEMCELL Technologies). A total of 4,400 progenitor cells were added to 2 ml MegaCult®-C media with cytokines. A volume of 1.2 ml cold collagen solution was then added. Then 0.75 ml of the final culture mixture was dispensed into each of the two wells of a double chamber slide. On day 12, cultures were dehydrated, fixed and stained for the detection of megakaryocyte progenitors.

### Megakaryocyte differentiation

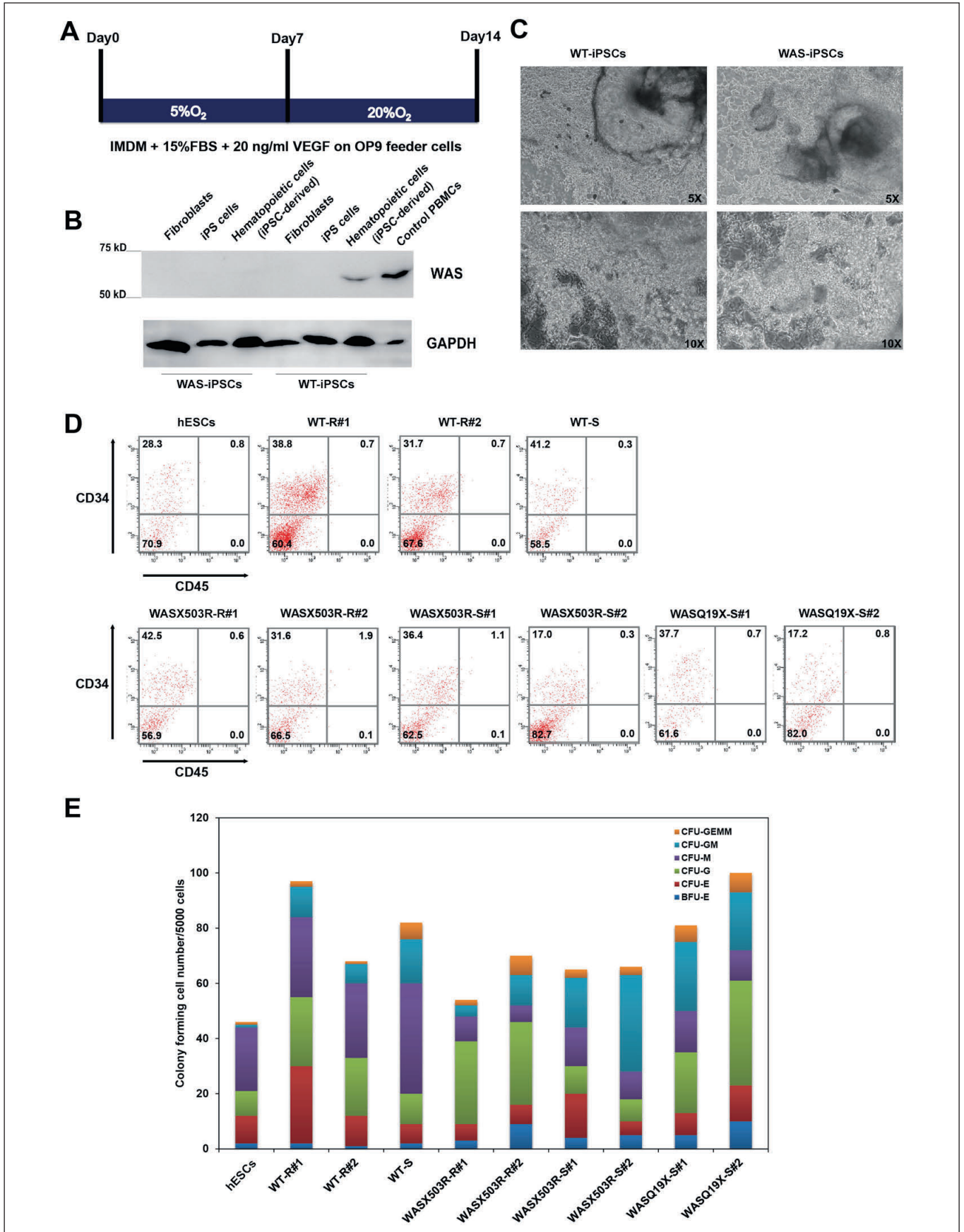
Human iPSCs were dissociated into small pieces (>100 cells) by collagenase treatment. Small clumps of human iPSCs were transferred onto mitotically inactivated OP9 cells and cultured in a haematopoietic cell differentiation medium, IMDM supplemented with a cocktail of 10  $\mu\text{g}/\text{ml}$  human insulin, 5.5  $\mu\text{g}/\text{ml}$  human transferrin, 5 ng/ml sodium selenite, 2 mM L-glutamine, 0.45 mM  $\alpha$ -monothioglycerol, 50  $\mu\text{g}/\text{ml}$  ascorbic acid, 15% FBS and 20 ng/ml human vascular endothelial growth factor (VEGF; R&D Systems, Minneapolis, MN, USA) (► Figure 1A). At 14 days after differentiation, cells were collected and gently crushed with a pipette and passed through a 40- $\mu\text{m}$  cell strainer to obtain haematopoietic progenitors, which were transferred onto freshly irradiated feeder cells and cultured in the haematopoietic cell differentiation medium supplemented with 50 ng/ml human thrombopoietin (TPO; R&D Systems), 10 ng/ml human stem cell factor (SCF; R&D Systems) and 25 ng/ml heparin (Sigma-Aldrich, St Louis, MO, USA). The non-adherent cells were collected and analysed on day 24.

### Flow cytometry analysis

Progenitor cells isolated from ES-sacs were stained with APC-conjugated anti-human CD34 (BD Biosciences, San Jose, CA, USA) and PerCP-conjugated anti-human CD45 (BD Biosciences) for haematopoietic cell analysis on day 14 of differentiation. FITC-conjugated anti-human CD41a (BioLegend) and PE-conjugated anti-human CD42b (BioLegend) were used to detect megakaryocyte differentiation and platelet-like particles. Stained cells were analysed by using BD FACSAria II (Becton Dickinson, Franklin Lakes, NJ, USA). For platelet analysis, platelet-like particles in culture supernatant were gated by using same FSC and SSC as normal platelet. The number of CD41a<sup>+</sup> CD42b<sup>+</sup> megakaryocytes and platelet-like particles was counted by using CountBright™ Absolute Counting Beads (Molecular Probes, Invitrogen).

### Electron microscopic (EM) analysis of human iPSC-derived megakaryocytes and platelets

Human iPSC-derived megakaryocytes and platelets were gently collected on day 24 as previously described (20). Briefly, one-ninth volume of acid citrate dextrose solution was added and centrifuged at 150 g for 10 min to collect megakaryocytes. The supernatant was transferred to a new tube. One  $\mu\text{M}$  prostaglandin E1 and 1 U/ml apyrase were added. The supernatant containing platelets was centrifuged at 400 g for 10 min to sediment the platelets.



Megakaryocytes and platelets were then fixed with 3% glutaraldehyde at 4°C for 60 min and post-fixed with 2% osmium tetroxide in phosphate buffer at 4°C for 60 min. Specimens were then dehydrated in ethanol and embedded in 100% resin at 60°C for 48 h. Thin sections were cut on an ultramicrotome and collected on mesh copper grids, stained with uranyl acetate and lead citrate. All images were examined by electron microscopy (JEOL 1210, JEOL, Tokyo, Japan). The shortest diameter of platelet particles containing alpha granules (A), dense core granules (D) and open canalicular systems (OCS) on whole mesh copper grid was measured by Image Pro Plus (Nikon, Tokyo, Japan).

## Results

### Derivation of iPSCs from WAS patients' fibroblasts

iPSCs were derived from fibroblasts obtained from two patients with WAS and from two unrelated control individuals by means of retroviral (30) or temperature-sensitive Sendai virus vectors (27) encoding Yamanaka's factors (OCT4, SOX2, KLF4, and c-MYC). Two control iPSC lines were generated using retrovirus (WT-R#1, 2) and one using Sendai virus (WT-S). For the WAS patient with c.1507T>A (p.X503R) (24), two iPSC lines were derived using retrovirus (WASX503R-R#1, 2) and two using Sendai virus (WASX503R-S#1, 2). Additional two iPSC lines were generated from the WAS patient with c.55C>T (p.Q19X) using Sendai virus (WASQ19X-S#1, 2) (25). Both patients exhibited classic WAS syndrome with complete lack of WASP expression. All nine iPSC lines maintained embryonic stem cell-like morphology, normal karyotype, and expressed pluripotency markers, OCT4, NANOG, TRA-1-60 and TRA-1-81 (see Suppl. Figure 1, available online at [www.thrombosis-online.com](http://www.thrombosis-online.com)). All SeV-iPSC lines were checked for the lack of residual SeV by immunofluorescence staining (see Suppl. Figure 2, available online at [www.thrombosis-online.com](http://www.thrombosis-online.com)). The pluripotency of all the iPSC lines was verified by teratoma formation assay (data not shown).

### Early haematopoietic development of WAS-iPSCs

WASP has been shown to be expressed in all haematopoietic cells as early as the stage of CD34<sup>+</sup> haematopoietic progenitors (15). To study the role WASP in early haematopoiesis, we compared the ability in the production of CD34<sup>+</sup> haematopoietic progenitors

through the ES-sac method among WAS-iPSCs, WT-iPSCs and human ESCs (► Figure 1A) (20, 21). While WASP levels were undetectable in dermal fibroblasts and undifferentiated iPSCs, WASP expression was found in haematopoietic cells differentiated from WT-iPSCs but not from WAS-iPSCs (► Figure 1B). After two weeks of co-culture with OP9 stromal cells and VEGF treatment (day 14), ES-sac like structures were observed from both WAS-iPSCs and WT-iPSCs (► Figure 1C). ES-sac derived CD34<sup>+</sup>/CD45<sup>-</sup> haemogenic endothelial cells were observed in all groups (► Figure 1D). The total number of haematopoietic progenitors capable of producing haematopoietic colonies on methylcellulose was not significantly different (► Figure 1E). All WAS-iPSC lines could give rise to most types of haematopoietic colonies including CFU-E, BFU-E, CFU-G, CFU-M, CFU-GM and CFU-GEMM. These data were similar to those obtained from earlier studies using CD34<sup>+</sup> from cord blood and bone marrow (14, 15) and suggested only minimal role of WASP in early haematopoiesis. Interestingly, all of the WAS-iPSC lines consistently produced fewer CFU-M colonies than the WT-iPSC lines in methylcellulose media (► Figure 1E). These results suggested potential defects in monocyte-granulocyte switching or monocyte survival/proliferation.

### Megakaryocyte differentiation

In order to test whether *in vitro* differentiation of iPSCs could be used to examine megakaryocytopoiesis and reproduce platelet defects observed in WAS, we first performed a megakaryocyte colony formation assay. ES-sacs from both groups were dissociated and 1,000 cells were cultured in collagen-based media supplemented with TPO and SCF. After 10 days of culture, the number of megakaryocyte colonies observed in all iPSC lines tested was not significantly different (► Figure 2A) suggesting that WASP did not play a major role up to the step of megakaryocyte progenitor production.

It is known that bone marrow microenvironment plays important roles in regulating megakaryocyte differentiation. To study whether WAS-iPSC-derived megakaryocytes exhibited defects during maturation, cells from ES-sacs were reseeded on OP9 marrow stromal cells (20, 21), and after 10 days of culture (day 24), the number of megakaryocytes was analysed by flow cytometry. We found that the percentage of megakaryocytes (CD41a<sup>+</sup>/42b<sup>+</sup>) within haematopoietic cells generated from WASX503R-R#1, 2 (75.6, 76.6, respectively) were slightly higher than other eight lines including hESCs (44.6%), WT-R#1 (63.4%), WT-R#2 (52.9%), WT-S (48.4%), WASX503R-S#1, 2 (50.6–64.0%), WASQ19X-S#1, 2 (52.6–63.8). To further characterise the megakaryocyte production, we performed a comparative time-course study of megakaryocyte differentiation from six iPSC lines on days 18, 21 and 24 (► Figure 2C). We observed a higher percentage of megakaryocytes (CD41a<sup>+</sup>/CD42b<sup>+</sup>) in cells differentiated from WASX503R-R#1, 2 on days 21 and 24 compared to other lines (► Figure 2C). Therefore WAS X503R-R#1, 2 appeared to stay in megakaryocyte stage longer than the rest.

**Figure 1: Haematopoietic differentiation of WAS-iPSCs.** A) Schematic diagram of *in vitro* differentiation protocol. B) Western blot analysis showing WASP expression in haematopoietic cells derived from WT-iPSCs (WT-R#1) but not in fibroblasts, iPSCs and haematopoietic cells derived from WAS-iPSCs (WASX503R-R#1). Peripheral blood mononuclear cells (PBMCs) expressing WASP were used as a control. C) Phase contrast photomicrographs of ES-sacs generated from WT-iPSCs and WAS-iPSCs on day 14; magnification 4X and 10X. D) Flow cytometry analysis of progenitor cells isolated from ES-sacs. CD34<sup>+</sup> CD45<sup>-</sup> haematopoietic progenitor cells were observed in all iPSC lines. E) The colony forming cell number of haematopoietic progenitors generated from human ESCs (CUHES), WT-iPSCs and WAS-iPSCs.

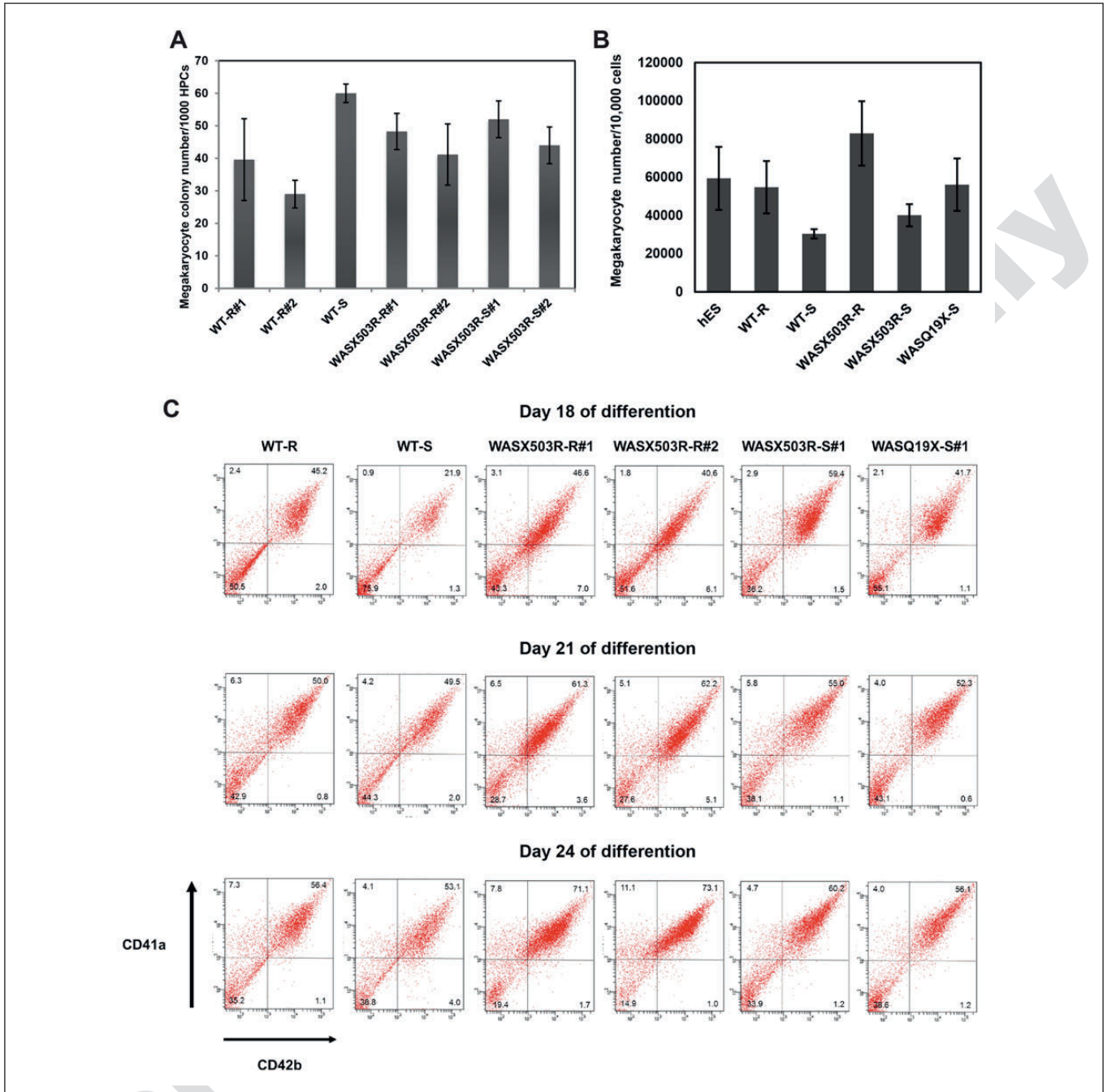


**Figure 2: WT-iPSCs and WAS-iPSCs generated similar numbers of megakaryocytes.** A) ES-sac derived HPCs on day 14 were cultured in Megacult media for 10 days. The resulting colonies were fixed, stained and counted. The number of megakaryocyte colonies observed in each group was not significantly different. Data were presented as mean  $\pm$  SEM, n=4. B) 10,000 ES-sac derived HPCs on day 14 were cultured on mitotically inactivated OP9 feeder cells with megakaryocyte differentiation media. Bar graph shows the total number of CD41+ and CD42+ megakaryocytes derived from

hESCs, WT-R#1, WT-S, WASX503R-R#1, WASX503R-S#1 and WASQ19X-S#1. Data are presented as mean  $\pm$  SEM, n=3. C) Flow cytometry analysis of megakaryocytes derived from WT-R, WT-S, WASX503R-R#1, WASX503R-R#2, WASX503R-S#1 and WASQ19X-S#1 on days 18, 21 and 24 using FITC-conjugated anti-human CD41a and PE-conjugated anti-human CD42b. There were higher percentages of megakaryocytes (CD41a+/CD42b+) in cells differentiated from WASX503R-R#1, 2 on days 21 and 24 compared to other lines.

Similar to previous reports (31, 32), the size of megakaryocytes derived from all iPSC and hESC lines in our studies was smaller than those generated from cord blood CD34<sup>+</sup> of healthy individuals. Electron microscopy analysis of megakaryocytes (day 24) demonstrated lower numbers of dense bodies in megakaryocytes derived from both lines of WASX503R-R. In addition, while well-developed demarcation membrane (DM) system was distributed throughout the cytoplasm of most megakaryocytes derived from the WT-R#1 (► Figure 3A), WT-S (► Figure 3B), WASX503R-S#1 (► Figure 3E), and WASQ19X-S#1 (► Figure 3F), the DM system could not be detected in most megakaryocytes derived from the WASX503R-R#1 (► Figure 3C). Very few megakaryocytes in this group contained poorly-developed DM system (► Figure 3D). These abnormalities were similar to what previously described in megakaryocytes from the peripheral blood and bone marrow of WAS patients (33, 34).

Since these defects were not observed in iPSCs generated with Sendai virus from both WAS patients, it is possible that the reprogramming method used could have a role in the above findings. Integrating reprogramming approaches including the use of retroviral vectors have been reported to increase immature megakaryocyte population possibly through transgene *c-MYC* reactivation (20). To test whether the lack of WASP also contributed to the phenotype we observed, we used lentivirus vectors to express WASP in the WASX503R-R#1. Interestingly, megakaryocytes derived from the WASX503R-R#1 with overexpression of WASP showed much improved DM system (see Suppl. Figure 3, available online at [www.thrombosis-online.com](http://www.thrombosis-online.com)) suggesting that WASP could also play a role in regulating distribution of DM system during megakaryocyte maturation.

### Platelet abnormalities generated from WAS-iPSCs

To measure the number of platelets produced from iPSC-derived megakaryocytes, supernatants containing platelet-like particles from megakaryocyte differentiation on day 24 were stained with anti-CD41a and CD42b. Platelet-like particles were counted by flow cytometry using the same forward light scatter (FSC) and side light scatter (SSC) for normal platelets (see Suppl. Figure 4, available online at [www.thrombosis-online.com](http://www.thrombosis-online.com)). Compared with WT-iPSCs, while the total number of platelet-like particles produced from all WASQ19X-S lines except WASQ19X-S#1 was not significantly different, all WASX503R lines produced fewer numbers of platelets (► Figure 4A). Electron microscopy analysis of platelet-like particles derived from the WASX503R-R#1, 2 showed irregular shapes with lower numbers of organelles and granules. Although platelet-like particles derived from all the WT-iPSCs and WAS-SeV-iPSCs revealed normal distribution of platelet granules, those from the WAS-SeV-iPSCs were small and had irregular shapes (► Figure 4B). The diameter of platelet-like particles derived from WASX503R-S#1 ( $1.927 \pm 0.934 \mu\text{m}$ ) and WASQ19X-S#1 ( $2.318 \pm 0.951 \mu\text{m}$ ) as measured under electron microscope was significantly smaller compared with the WT-R#1 ( $3.234 \pm 0.860 \mu\text{m}$ ) and WT-S#1 ( $2.665 \pm 0.852 \mu\text{m}$ ) ( $p < 0.001$ ). Thus, WAS-iPSCs produced small and irregular-sized platelets, the hallmark of WAS.

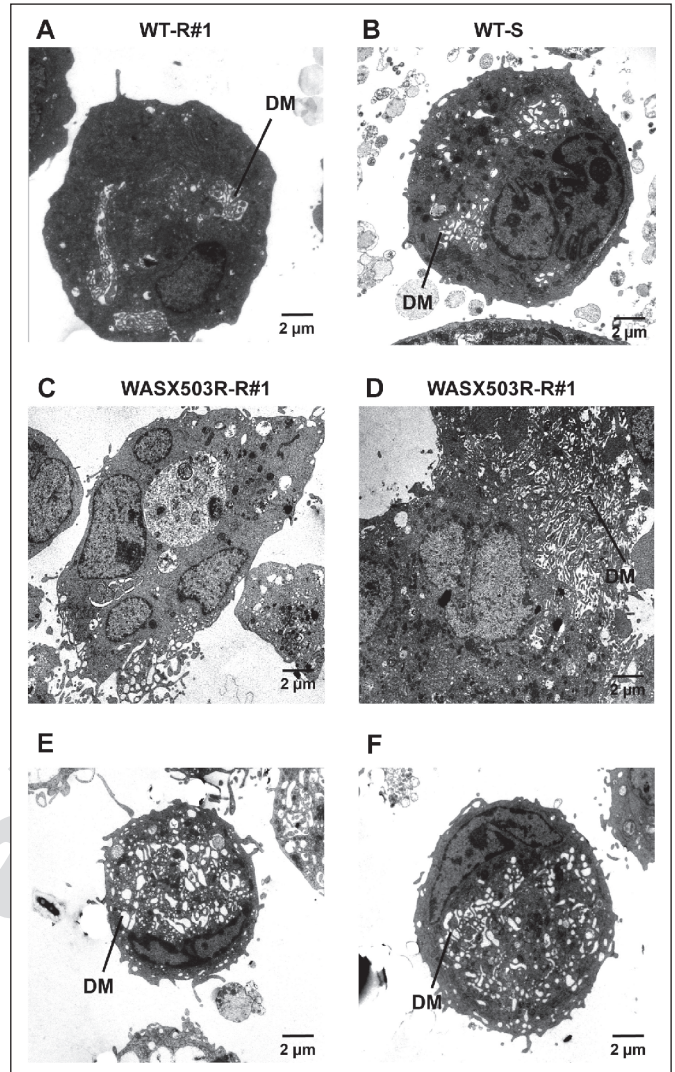


**Figure 3: Megakaryocytes generated from WAS-iPSCs.** Electron microscopic examination of megakaryocytes generated from WT-R#1, WT-S, WASX503R-R#1, WASX503R-S#1 and WASQ19X-S#1 derived megakaryocytes. Demarcation membrane system (DM) within the cytoplasm was observed in megakaryocytes derived from all iPSC lines. Notably, DM of megakaryocytes derived from WASX503R-R#1 was rarely observed. The abnormality of demarcation membrane system was seen as small-sized fragments throughout the cytoplasm of megakaryocytes (left). WASX503R-R#1 derived megakaryocytes also demonstrated lower organelle contents within cytoplasm compared to the WT control (right).

### Defects in proplatelet formation in megakaryocytes derived from WAS-iPSCs

When co-cultured with OP9 stromal cells, the hESCs, WT-R, and WT-S generated several proplatelet clusters with long extension. We could not detect proplatelet clusters in the WASX503R-R group. Although proplatelets could be rarely observed in the WASX503R-S#1, they were morphologically distinct from the WT group. Proplatelet processes were much shorter and less complex. The WASQ19X-S#1 produced more proplatelets than the

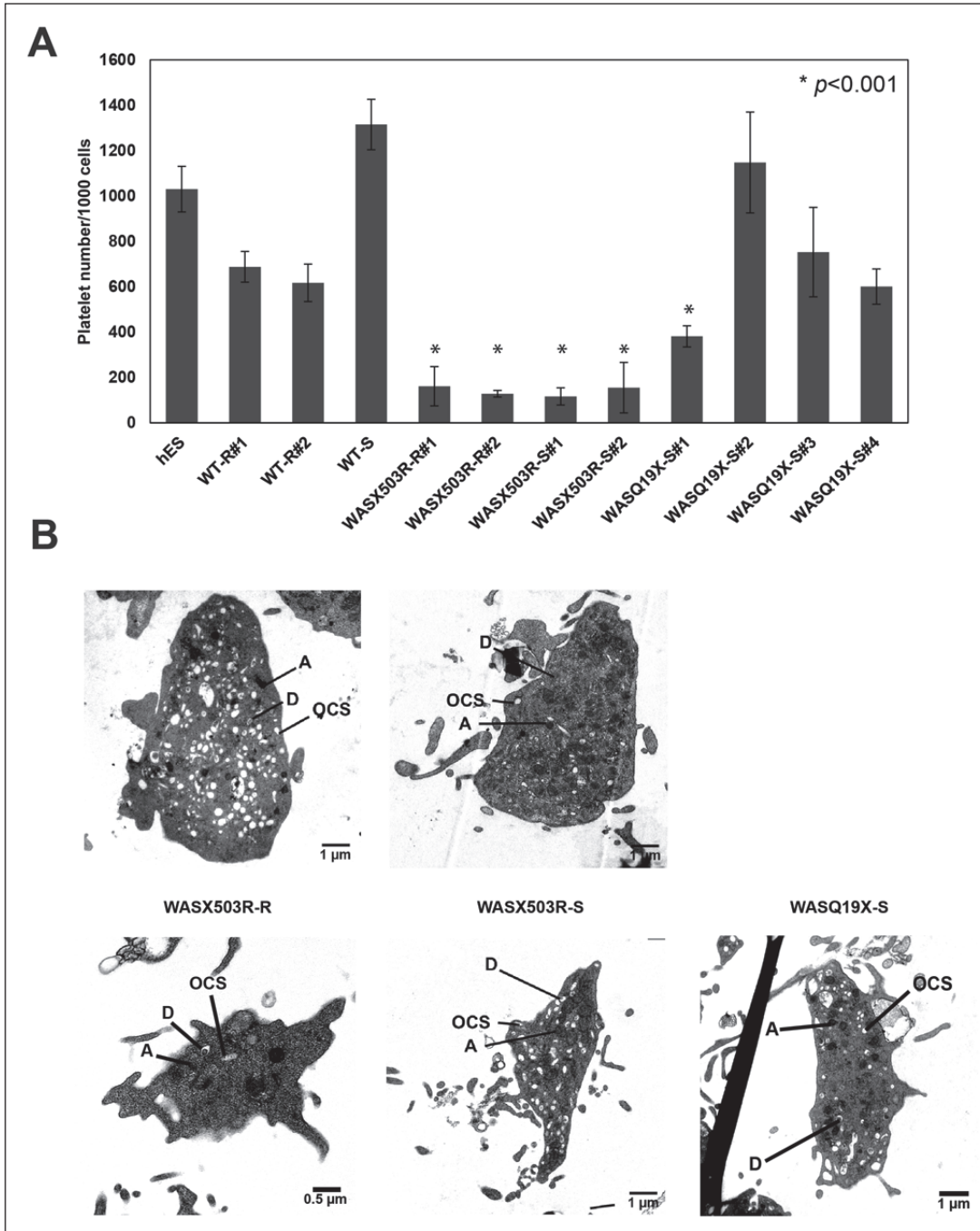


**Figure 4: WAS-iPSC-derived platelets.** A) Bar graph showing the number of platelet-like particles generated from hESCs, WT-R, WT-S, WASX503R-R, WASX503R-S and WASQ19X-S. Data are presented as mean  $\pm$  SEM,  $n=5$ . The asterisks (\*) denote the results that are significantly different ( $p < 0.001$ ) from those obtained from the WT-iPSCs. B) Transmission electron micrograph showing ultrastructure of platelet-like particles obtained from WT-R#1, WT-S, WASX503R-R#1, WASX503R-S#1 and WASQ19X-S#1. Platelet-like particles derived from WT-R#1, WT-S, WASX503R-S#1 and WASQ19X-S#1 demonstrated several organelles including dense body (D), alpha granule (A) and open canalicular system (OCS) throughout the cytoplasm of platelet-like particles. Platelet-like particles obtained from WASX503R-R#1 had non-discoid shapes with lower numbers of platelet organelles and granules.

WASX503R-S#1 but they shared the same abnormal morphology (► Figure 5A). To further quantify the number of proplatelet forming cells, 1,000 cells from day 21 of the OP9 co-culture were plated into each well of 96-well plates and proplatelet clusters were counted on days 1, 3, and 5 after plating.

Although we observed proplatelet forming cells at the mean of 18, 31, and 14 out of 1,000 seeding cells on days 22, 24, and 26, respectively, in the WT-R group, proplatelet forming cells were undetectable in the WASX503R-R and significantly lower in the WASX503R-S. All the WASQ19X-S lines produced proplatelet

clusters with the number close to the WT group. However their morphology was markedly worse than the control (► Figure 5 and Suppl. Figure 5, available online at [www.thrombosis-online.com](http://www.thrombosis-online.com)).

Some previous studies showed that  $CD34^+$  from WAS patients could form proplatelets normally in the feeder-free condition (16). The iPSC-derived megakaryocytes (day 21) were dissociated from feeders and plated on matrigel-coated slides, and allowed to differentiate for 24 h. Under this condition, proplatelet forming cells could be detected in all lines. Nevertheless, immunofluorescence staining of  $\alpha$ -tubulin demonstrated that proplatelet processes ex-

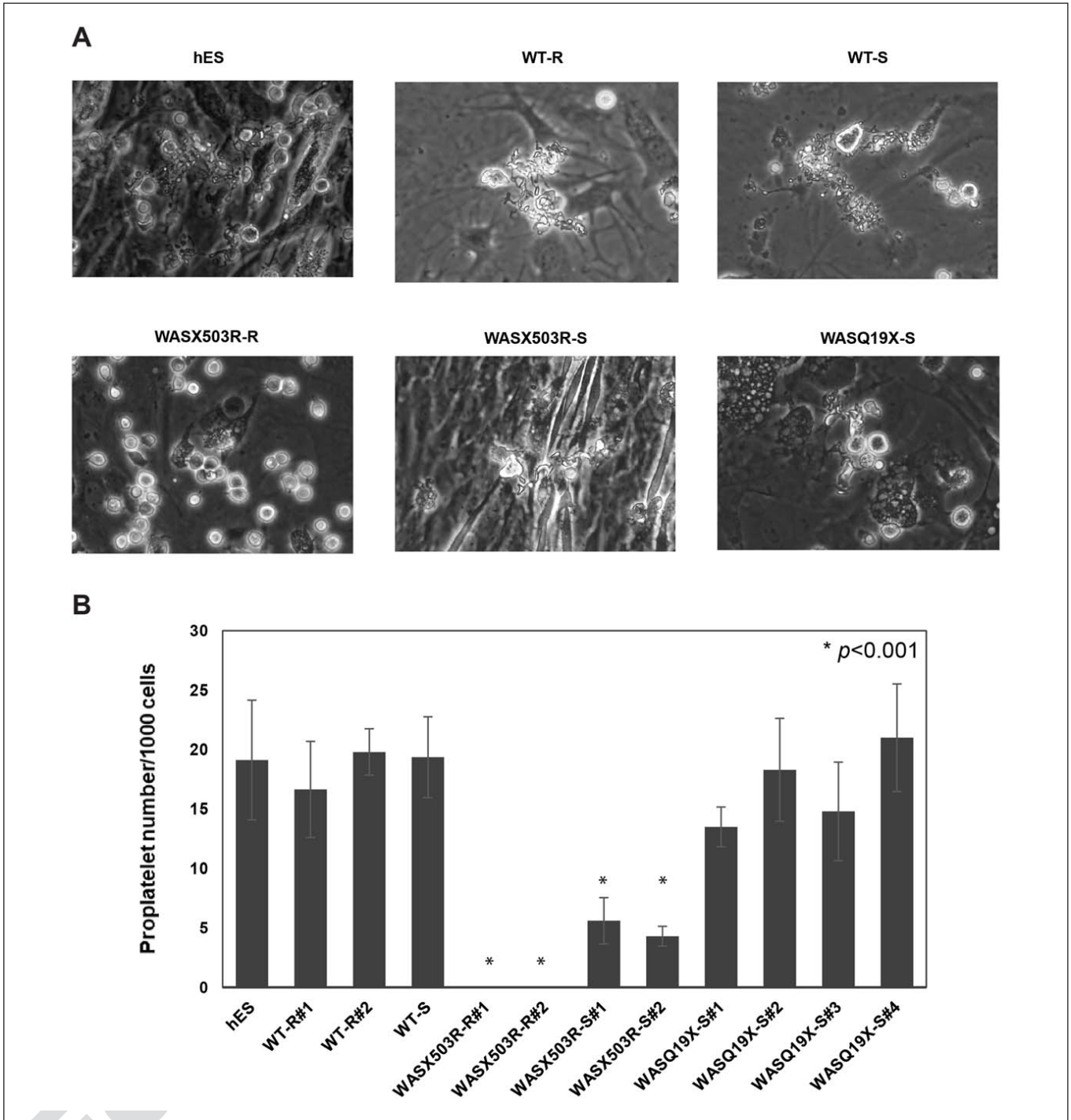


**Figure 5: Proplatelet formation in megakaryocytes derived from WAS-iPSCs.** A) Phase contrast images of megakaryocytes derived from hESCs, WT-R#1, WT-S, WASX503R-R#1, WASX503R-S#1 and WASQ19X-S#1. Proplatelet formation was detected in hESCs, WT-R#1, WT-S, WASX503R-S#1 and WASQ19X-S#1 derived megakaryocytes. Proplatelet arm extension of WASX503R-S#1 and WASQ19X-S#1 derived megakaryocytes was shorter than that of the WT group. B) On day 21 of differentiation, 1,000 iPSC-

derived megakaryocytes were reseeded on mitotically inactivated OP9 feeder cells. The number of proplatelet forming cells was counted on day 22. Data are presented as mean  $\pm$  SEM,  $n=5$ . Proplatelet forming cells were detected in the hESCs, WT-R, WT-S, WASX503R-S and WASQ19X-S derived megakaryocytes while they were undetectable at any time point in the WASX503R-R. The asterisks (\*) denote the results that are significantly different ( $p < 0.001$ ) from those obtained from the WT-iPSCs.

tended from most megakaryocytes derived from both patients (WASX503R-S and WASQ19X-S) were remarkably thinner and showed less branching than the WT control (► Figure 6A). Overexpression of WASP increased branching and length of proplatelet extension (► Figure 6B). Without feeders, the number of proplatelet forming cells was higher in all groups (► Figure 6C). The mean size of WAS-iPSC-derived platelets as measured from the diameter of tubulin-stained discoid-shaped platelets was significantly smaller than the control (► Figure 6D, E). In addition, overexpression of WASP in the WASQ19X-S increased the mean platelet size (► Figure 6D, E). These data support the role of WASP in regulating cytoskeletal rearrangement during proplatelet extension and controlling the platelet size.

### Defects in cytoskeleton reorganisation

To test whether megakaryocytes from the WAS-iPSCs exhibited defects in actin cytoskeleton, megakaryocytes derived from all iPSC lines were seeded on type I collagen-coated coverslips and stained for F-actin using phalloidin. While F-actin polymerisation was observed in the periphery of the WT-iPSC-derived megakaryocytes, it was absent in the WAS-iPSC-derived megakaryocytes (► Figure 7). Time-lapse analysis following megakaryocyte attachment for two days excluded the possibility of delayed reorganisation (data not shown). All these data suggested that the *in vitro* platelet production system studied in iPSCs could recapitulate abnormalities in thrombopoiesis identified in WAS patients.

## Discussion

In this study we report on the generation of WAS-iPSC lines and demonstrate that *in vitro* differentiation can produce megakaryocytes and platelets with disease-associated phenotypes. We have also shown that megakaryocytes derived from the WAS-iPSCs exhibit defects in F-actin localisation and proplatelet formation. The WAS-iPSCs can be used to elucidate the role of WASP in different blood cell lineages and to optimise gene correction strategies for therapeutic application.

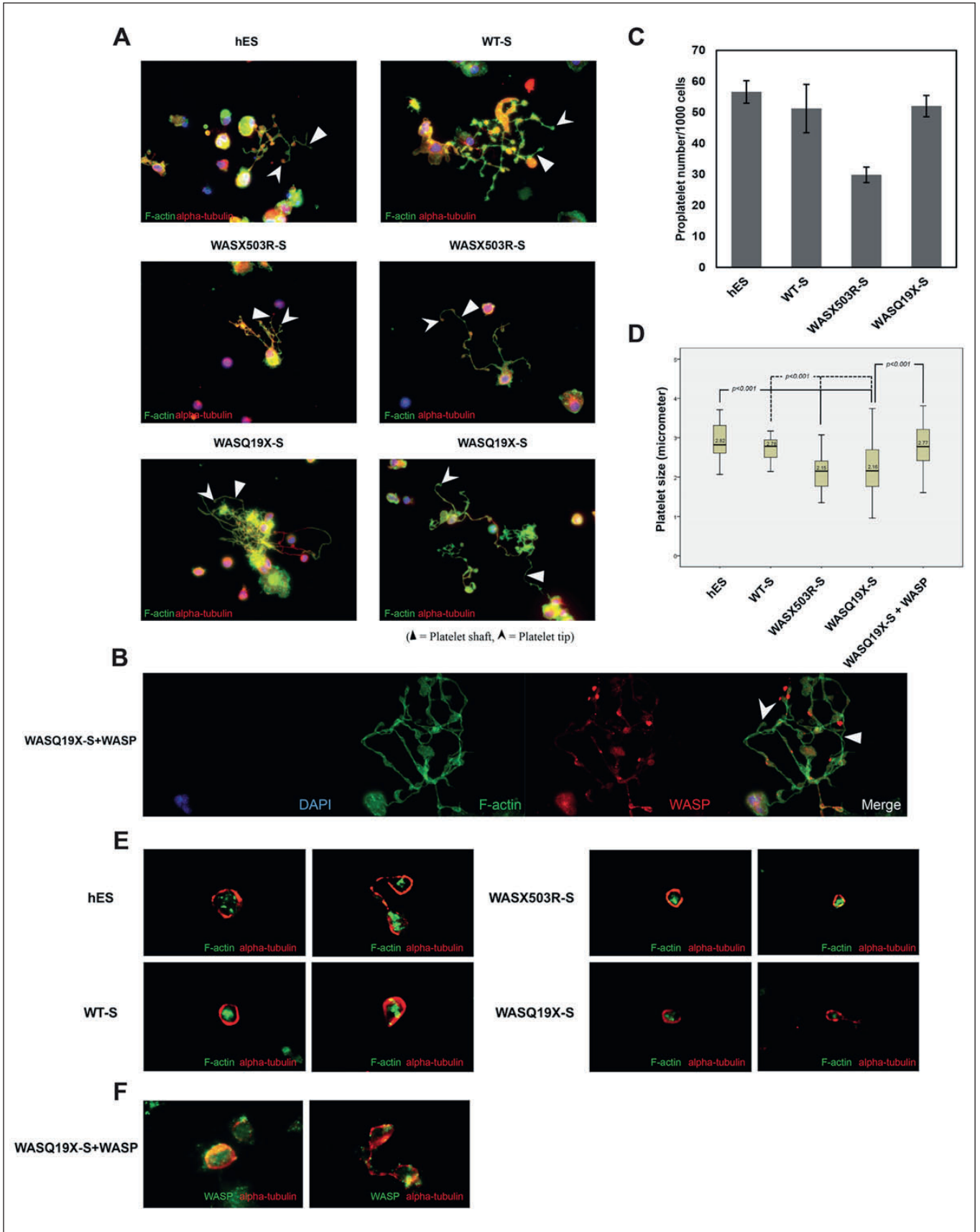
The finding that there were no significant differences among the WAS-iPSC, normal iPSC, and hESC lines in generating most haematopoietic lineages was consistent with the clinical findings of WAS patients having no obvious defects in haematopoiesis (8). One potential defect we observed was the persistent reduction in the percentage of CFU-M and an increase in proportion of cells giving rise to CFU-GM. This suggested that WASP could play a role in the lineage decision between neutrophils and monocytes. It might also help explain why activating mutations in WASP cause congenital neutropenia (35). Further studies are required to address this issue.

We observed an abnormal pattern of F-actin distribution in WAS-iPSC-derived megakaryocytes when contacted with collagen similar to what previously described in megakaryocytes derived from CD34+ cells from bone marrow by Haddad et al. Instead of peripheral distribution under the cytoplasmic membrane, F-actin

was localised towards the centre of the WAS-iPSC-derived megakaryocytes. The actin-rich peripheral zone has been proposed to prevent microtubule invasion and premature proplatelet process extension (36, 37). While in some previous studies no proplatelet defects were detected, we observed abnormal proplatelet processes from megakaryocytes derived from all WAS-iPSC lines generated from our two patients. Remarkably, the thin, less branching, proplatelet processes extended from WAS-iPSC-derived megakaryocytes were similar to what observed in megakaryocytes treated with actin-disrupting agents cytochalasin B, and D (36–38). Thus, our results support the role of WASP in regulating F-actin cytoskeletal rearrangement during megakaryocyte maturation. It is possible that in the inhibitory environment of bone marrow, abnormal distribution of actin filaments resulted from defective WASP could lead to premature fragmentation similar to what has been demonstrated in a mouse model.

The model that megakaryocytes produced platelets through the step of proplatelet formation was confirmed by an elegant study revealing proplatelet-like structures extended from megakaryocytes into sinusoidal blood vessels *in vivo* (39). Fluid shear stress is likely to play an important role in proplatelet extension and determination of final platelet size *in vivo* (40). Although there was no fluid flow in our *in vitro* differentiation system, WAS-iPSC-derived megakaryocytes produced smaller tubulin-stained, discoid-shaped platelet-like particles compared to the control consistent with small bead size found at the proplatelet tips. Overexpression of WASP in WAS-iPSC-derived megakaryocytes improved the branching of proplatelets and increased the mean platelet size. Thus, small-sized platelets found in our WAS patients could be, in

**Figure 6: WAS-iPSC-derived megakaryocytes showed abnormal proplatelet structures in the feeder free condition.** On day 21 of differentiation, iPSC-derived megakaryocytes were reseeded on matrigel-coated coverslips and cultured for 24 h. Proplatelet forming cells were fixed and stained with anti- $\alpha$ -tubulin (red) and phalloidin-FITC (green). A) WASX503R-S#1- and WASQ19X-S#1-derived megakaryocytes showed abnormal proplatelet structures with small-sized platelet particles at the end of the proplatelet tip compared to the WT control (magnification 40X). B) WASQ19X-S#1-derived megakaryocytes were transduced with lentiviruses expressing WASP (WASQ19X-S#1+WASP). WASQ19X-S#1+WASP-derived proplatelets stained with anti- $\alpha$ -tubulin (red) and anti-WASP (green) showed thicker proplatelet shafts with numerous platelet particles (magnification 100X). C) On day 21 of differentiation, 1,000 iPSC-derived megakaryocytes were reseeded on the matrigel-coated plate. The number of proplatelet forming cells was counted on day 22. Data are presented as mean  $\pm$  SEM, n=5. The number of proplatelet-forming cells detected in hESCs-, WT-S-, WASX503R-S#1- and WASQ19X-S#1-derived megakaryocytes were higher compared to that in cells cultured in the OP9 feeder condition. D) A box plot showing the diameter of tubulin-stained discoid-shaped platelets generated from hESCs, WT-S, WASX503R-S#1, WASQ19X-S#1 and WASQ19X-S#1+WASP. Data are presented as mean  $\pm$  SEM, n=31. The asterisks (\*) denote the results that are significantly different ( $p < 0.001$ ) from those obtained from the WT-iPSCs. E) Immunofluorescence staining of platelet particles (magnification 100X). The platelet particles were stained with anti- $\alpha$ -tubulin (red) and phalloidin-FITC (green). WASQ19X-WASP-derived platelets were stained with anti- $\alpha$ -tubulin (red) and anti-WASP (green).



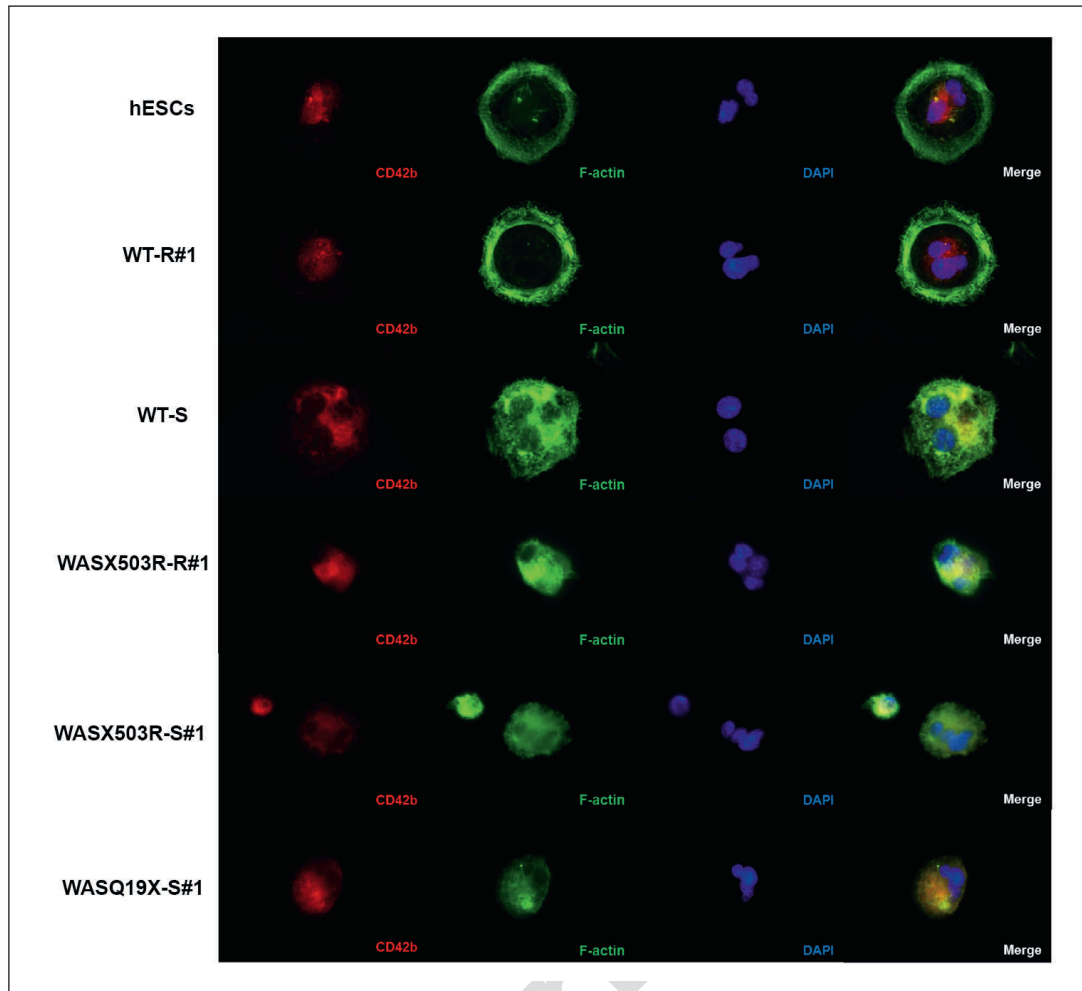


**Figure 7: Cytoskeleton reorganisation in megakaryocytes derived from WAS-iPSCs.** Immunofluorescence staining of megakaryocytes derived from hESCs, WT-R#1, WT-S, WASX503R-R#1, WASX503R-S#1 and WASQ19X-S#1 using phalloidin-FITC (green) and anti CD42b-PE (red) demonstrating that all WT-iPSC-derived megakaryocytes retained normal actin polymerisation. DAPI (blue) was used for nuclear staining (magnification 100X).

part, caused by defects in WASP function in regulating cytoskeletal protein rearrangement during proplatelet extension. Since normal proplatelet formation was documented in some previous reports (16), there could be heterogeneity among WAS patients. In our system all cell lines generated from the WAS patient with the X503R mutation showed more severe defects than those from the WAS patient with the Q19X mutation suggesting that genetic background could influence the phenotypic severity. Further studies using isogenic iPSC lines in combination with genome editing technologies such as TALENs and CRISPR/Cas9 could lead to a better understanding of the factors regulating thrombopoiesis.

Although we found a quantitative defect in platelet production in five out of eight WAS-iPSC lines we tested, this finding could not entirely explain thrombocytopenia found in WAS patients. The fragile and limited proplatelet structure observed in our study suggested that some of the platelets produced from WAS-iPSC-derived megakaryocytes might not be able to enter the circulation *in vivo*. The abnormal platelet structure could also increase its vulnerability. Because splenectomy could increase the number of platelets in most cases of WAS patients, peripheral destruction is likely to be another important contributing factor for thrombocytopenia.

Although unlimited self-renewal capability of iPSCs enables repetitive studies of cells from patients with rare diseases, there are special concerns when interpreting results of iPSC studies. Residual epigenetic memory from parental somatic cells and the reprogramming method could affect their differentiation potentials resulted in interline variability (3, 41). The phenotype observed in each patient may be influenced by epigenetic changes caused by aging and various exposures. Since cell reprogramming can erase the epigenetic state of starting cells, the iPSC model may or may not exhibit corresponding disease phenotype.

In our study, we cannot exclude the possibility that retroviral vectors used in iPSC generation contribute to defects in megakaryocyte differentiation that we observed in WASX503R#1-2. It has previously been shown that high levels of the reprogramming factor *c-Myc* could promote megakaryocyte proliferation without maturation (20, 42). Reactivation of transgene *myc* could happen in cells reprogrammed with viral vectors that integrate into the genome of host cells.

Even though our RT-PCR demonstrated that *c-MYC* transgene was silenced in both WT-R#1, 2 and WASX503R-R#1, 2 (see Suppl. Figure 3A, available online at [www.thrombosis-online.com](http://www.thrombosis-online.com)) and epigenetic studies of the endogenous *Oct4* promoter suggested

a similar degree of reprogramming (see Suppl. Figure 3B, available online at [www.thrombosis-online.com](http://www.thrombosis-online.com)). There is still a possibility that reactivation of the transgene cassette during megakaryocyte differentiation might occur. Remarkably, the WAS-R but not the WT-R produced megakaryocytes with abnormal demarcation membrane system and platelet-like particles with reduced granules. These ultrastructural defects were similar to those found in an early study of WAS (33). Overexpression of WASP improved demarcation membrane distribution and increased platelet contents in megakaryocytes and platelets derived from the WAS-R (see Suppl. Figure 3C, D, available online at [www.thrombosis-online.com](http://www.thrombosis-online.com)) suggesting that WASP could play a role in this process. Nevertheless, as we were unable to detect these defects in all megakaryocytes and platelets derived from the WAS-S lines, we concluded that lack of WASP alone was not sufficient to cause these changes. It is possible that bone marrow microenvironment of WAS patients could provide additional factor(s) to enhance such changes. Several signalling molecules found in the bone marrow, such as Wnt, TGF- $\beta$ , NF- $\kappa$ B and IL-6 are known to be important regulators of the c-MYC promoter (43). The levels of these signal molecules can change dramatically during stress and other pathological conditions. It would be interesting to see whether these signals could induce these abnormalities in cells derived from WAS-iPSC-S lines or WAS-CD34+ from cord blood/ bone marrow.

Restoring immune cell functions normally requires allogeneic haematopoietic stem cell transplantation, the only curative therapy for WAS. The difficulty in finding HLA-matched donors and complications related to transplantation urge the development of gene therapy strategies for WAS. Haematopoietic stem cell gene therapy using retroviral and lentiviral vectors has shown to restore natural killer, T and B cell functions both in mouse models (44, 45) and in two patients with WAS (46). Even though the lentiviral vectors used in our study was not optimised, we could observe an improvement in megakaryocyte and platelet phenotypes. Therefore, WAS-iPSCs could be used for optimising gene therapy strategies and screening for effective therapeutic agents for WAS. A recent study demonstrated that zinc finger nuclease (ZFN)-mediated gene targeting at the AAVS1 site of iPSCs from patients with X-linked chronic granulomatous disease led to more sustained expression of gp91<sup>phox</sup> and functional correction of neutrophils comparing to transduction with self-inactivating lentiviral vectors expressing gp91<sup>phox</sup> under the EF1 $\alpha$  promoter (47). We are currently evaluating the ZFN and TALEN strategies in correction of the disease phenotype and comparing the effects between ZFN targeting at the AAV1 site and ZFN-mediated gene correction by homologous recombination in WASP.

We have successfully validated that the WAS-iPSC model could recapitulate WAS disease phenotypes and demonstrated the significant role of WASP in platelet production. We also showed that overexpression of WASP in the WAS-iPSCs could lead to phenotypic rescue. Recently, it has been demonstrated that transplantable human haematopoietic stem cells can be generated from human iPSCs (48). With the improvement in techniques for generating clinical-grade haematopoietic stem cells from pluripotent stem cells and advances in gene targeting strategies, gene-cor-

### What is known about this topic?

- Wiskott-Aldrich syndrome (WAS) is caused by mutations in the gene encoding WAS protein (WASP). The WASP is expressed in all hematopoietic lineages and participates in the re-organisation of actin cytoskeleton of hematopoietic and immune cells in response to extra-cellular stimuli.
- While the patients with WAS have microthrombocytopenia, mice with WASP deficiency exhibit only mild thrombocytopenia with normal-sized platelets.
- Previous studies in humans have provided different results. While some studies revealed that mutations in the WASP gene resulted in defects of megakaryocyte generation and differentiation, others demonstrated that megakaryocytes from WAS patients could mature and form proplatelet normally. In addition, the number of megakaryocytes in the bone marrow of WAS patients was usually found to be normal.

### What does this paper add?

- Induced pluripotent stem cells generated from patients with WAS (WAS-iPSCs) could produce megakaryocytes and platelets with WAS phenotypes.
- Cytoskeletal rearrangements and proplatelet formation were impaired in cells derived from WAS-iPSCs.
- WAS-iPSCs exhibited defects in platelet production *in vitro* and produced platelets with more irregular shapes and smaller sizes. Overexpression of WASP using a lentiviral vector improved proplatelet structures and increased the platelet size.

rected haematopoietic stem/progenitor cells derived from the patient iPSCs may one day become a viable alternative for treatment of severe immune deficiency diseases.

### Acknowledgements

We thank Dr. Chatchatee and Dr. Suratannon for providing excellent patient care, Dr. Nanakorn and Dr. Rojnuckarin for technical advices, and Dr. Nakauchi and Dr. Otsu for helpful advices on platelet differentiation. This study was supported by co-funding of the Royal Golden Jubilee Ph.D. Program and Chulalongkorn University to PA (Grant No. PHD/0202/2552), the National Science and Technology Development Agency, the Thailand Research Fund, and the National Research University Project, Office of the Higher Education Commission (HR1166I and HR1163A) and Ratchadapiseksomphot Endowment Fund of Chulalongkorn University (RES560530177-HR).

### Author contributions

P.I., and P.A.: collection and/or assembly of data, data analysis and interpretation, and manuscript writing. R.R., S.M.L, and D.S.: collection and/or assembly of data and data analysis and interpretation. K.S., N.I., and V.S.: conception and design, data analysis and interpretation, financial support, manuscript writing, and final approval of the manuscript.

## Conflicts of interest

None declared.

## References

1. Takahashi K, Yamanaka S. Induction of pluripotent stem cells from mouse embryonic and adult fibroblast cultures by defined factors. *Cell* 2006; 126: 663–676.
2. Lee G, Papapetrou EP, Kim H, et al. Modelling pathogenesis and treatment of familial dysautonomia using patient-specific iPSCs. *Nature* 2009; 461: 402–406.
3. Marchetto MC, Carroumeu C, Acab A, et al. A model for neural development and treatment of Rett syndrome using human induced pluripotent stem cells. *Cell* 2010; 143: 527–539.
4. Moretti A, Bellin M, Welling A, et al. Patient-specific induced pluripotent stem-cell models for long-QT syndrome. *N Engl J Med* 2010; 363: 1397–1409.
5. Grskovic M, Javaherian A, Strulovici B, et al. Induced pluripotent stem cells—opportunities for disease modelling and drug discovery. *Nat Rev Drug Discov* 2011; 10: 915–929.
6. Onder TT, Daley GQ. New lessons learned from disease modeling with induced pluripotent stem cells. *Curr Opin Genetics Devel* 2012; 22: 500–508.
7. Orange JS, Stone KD, Turvey SE, et al. The Wiskott-Aldrich syndrome. *Cell Mol Life Sci* 2004; 61: 2361–2385.
8. Thrasher AJ, Burns SO. WASP: a key immunological multitasker. *Nat Rev Immunol* 2010; 10: 182–192.
9. Snapper SB, Rosen FS. The Wiskott-Aldrich syndrome protein (WASP): roles in signaling and cytoskeletal organisation. *Ann Rev Immunol* 1999; 17: 905–929.
10. Taylor MD, Sadhukhan S, Kottangada P, et al. Nuclear role of WASp in the pathogenesis of dysregulated TH1 immunity in human Wiskott-Aldrich syndrome. *Sci Transl Med* 2010; 2: 37ra44.
11. Moulding DA, Blundell MP, Spiller DG, et al. Unregulated actin polymerisation by WASp causes defects of mitosis and cytokinesis in X-linked neutropenia. *J Exp Med* 2007; 204: 2213–2224.
12. Devriendt K, Kim AS, Mathijs G, et al. Constitutively activating mutation in WASP causes X-linked severe congenital neutropenia. *Nat Genet* 2001; 27: 313–317.
13. Snapper SB, Rosen FS, Mizoguchi E, et al. Wiskott-Aldrich syndrome protein-deficient mice reveal a role for WASP in T but not B cell activation. *Immunity* 1998; 9: 81–91.
14. Sabri S, Foudi A, Boukour S, et al. Deficiency in the Wiskott-Aldrich protein induces premature proplatelet formation and platelet production in the bone marrow compartment. *Blood* 2006; 108: 134–140.
15. Kajiwaru M, Nonoyama S, Eguchi M, et al. WASP is involved in proliferation and differentiation of human haemopoietic progenitors in vitro. *Br J Haematol* 1999; 107: 254–262.
16. Haddad E, Cramer E, Riviere C, et al. The thrombocytopenia of Wiskott Aldrich syndrome is not related to a defect in proplatelet formation. *Blood* 1999; 94: 509–518.
17. Woods NB, Parker AS, Moraghebi R, et al. Brief report: efficient generation of haematopoietic precursors and progenitors from human pluripotent stem cell lines. *Stem Cells* 2011; 29: 1158–1164.
18. Vodyanik MA, Bork JA, Thomson JA, et al. Human embryonic stem cell-derived CD34+ cells: efficient production in the coculture with OP9 stromal cells and analysis of lymphohaematopoietic potential. *Blood* 2005; 105: 617–626.
19. Kaufman DS, Hanson ET, Lewis RL, et al. Haematopoietic colony-forming cells derived from human embryonic stem cells. *Proc Natl Acad Sci USA* 2001; 98: 10716–10721.
20. Takayama N, Nishimura S, Nakamura S, et al. Transient activation of c-MYC expression is critical for efficient platelet generation from human induced pluripotent stem cells. *J Exp Med* 2010; 207: 2817–2830.
21. Takayama N, Nishikii H, Usui J, et al. Generation of functional platelets from human embryonic stem cells in vitro via ES-sacs, VEGF-promoted structures that concentrate haematopoietic progenitors. *Blood* 2008; 111: 5298–5306.
22. Lu SJ, Li F, Yin H, et al. Platelets generated from human embryonic stem cells are functional in vitro and in the microcirculation of living mice. *Cell Res* 2011; 21: 530–545.
23. Takayama N, Eto K. Pluripotent stem cells reveal the developmental biology of human megakaryocytes and provide a source of platelets for clinical application. *Cell Mol Life Sci* 2012; 69: 3419–3428.
24. Chatchatee P, Srichomthong C, Chewatavorn A, et al. A novel termination codon mutation of the WAS gene in a Thai family with Wiskott-Aldrich syndrome. *Int J Mol Med* 2003; 12: 939–941.
25. Amarinthukrowh P, Ittiporn S, Tongkobpetch S, et al. Clinical and molecular characterisation of Thai patients with Wiskott-Aldrich syndrome. *Scand J Immunol* 2013; 77: 69–74.
26. Fusaki N, Ban H, Nishiyama A, et al. Efficient induction of transgene-free human pluripotent stem cells using a vector based on Sendai virus, an RNA virus that does not integrate into the host genome. *Proc Jpn Acad Ser B Phys Biol Sci* 2009; 85: 348–362.
27. Ban H, Nishishita N, Fusaki N, et al. Efficient generation of transgene-free human induced pluripotent stem cells (iPSCs) by temperature-sensitive Sendai virus vectors. *Proc Natl Acad Sci USA* 2011; 108: 14234–14239.
28. Nishishita N, Shikamura M, Takenaka C, et al. Generation of virus-free induced pluripotent stem cell clones on a synthetic matrix via a single cell subcloning in the naive state. *PLoS One* 2012; 7: e38389.
29. Pruksananonda K, Rungsiwut N, Numchairsika P, et al. Eighteen-year cryopreservation does not negatively affect the pluripotency of human embryos: evidence from embryonic stem cell derivation. *Biores Open Access* 2012; 1: 166–173.
30. Park IH, Zhao R, West JA, et al. Reprogramming of human somatic cells to pluripotency with defined factors. *Nature* 2008; 451: 141–146.
31. Reems JA, Pineault N, Sun S. In vitro megakaryocyte production and platelet biogenesis: state of the art. *Transfus Med Rev* 2010; 24: 33–43.
32. Gekas C, Graf T. Induced pluripotent stem cell-derived human platelets: one step closer to the clinic. *J Exp Med* 2010; 207: 2781–2784.
33. Grottum KA, Hovig T, Holmsen H, et al. Wiskott-Aldrich syndrome: qualitative platelet defects and short platelet survival. *Br J Haematol* 1969; 17: 373–388.
34. Luthi JN, Gandhi MJ, Drachman JG. X-linked thrombocytopenia caused by a mutation in the Wiskott-Aldrich syndrome (WAS) gene that disrupts interaction with the WAS protein (WASP)-interacting protein (WIP). *Exp Hematol* 2003; 31: 150–158.
35. Ancliff PJ, Blundell MP, Cory GO, et al. Two novel activating mutations in the Wiskott-Aldrich syndrome protein result in congenital neutropenia. *Blood* 2006; 108: 2182–2189.
36. Leven RM, Yee MK. Megakaryocyte morphogenesis stimulated in vitro by whole and partially fractionated thrombocytopenic plasma: a model system for the study of platelet formation. *Blood* 1987; 69: 1046–1052.
37. Tablin F, Castro M, Leven RM. Blood platelet formation in vitro. The role of the cytoskeleton in megakaryocyte fragmentation. *J Cell Sci* 1990; 97: 59–70.
38. Italiano JE, Jr., Lecine P, Shivdasani RA, et al. Blood platelets are assembled principally at the ends of proplatelet processes produced by differentiated megakaryocytes. *J Cell Biol* 1999; 147: 1299–1312.
39. Junt T, Schulze H, Chen Z, et al. Dynamic visualisation of thrombopoiesis within bone marrow. *Science* 2007; 317: 1767–1770.
40. Thon JN, Macleod H, Begonja AJ, et al. Microtubule and cortical forces determine platelet size during vascular platelet production. *Nat Commun* 2012; 3: 852.
41. Kim K, Doi A, Wen B, et al. Epigenetic memory in induced pluripotent stem cells. *Nature* 2010; 467: 285–290.
42. Thompson A, Zhao Z, Ladd D, et al. A new transgenic mouse model for the study of cell cycle control in megakaryocytes. *Stem Cells* 1996; 14 (Suppl 1): 181–187.
43. Liu J, Levens D. Making myc. *Curr Top Microbiol Immunol* 2006; 302: 1–32.
44. Astrakhan A, Sather BD, Ryu BY, et al. Ubiquitous high-level gene expression in haematopoietic lineages provides effective lentiviral gene therapy of murine Wiskott-Aldrich syndrome. *Blood* 2012; 119: 4395–4407.
45. Bosticardo M, Draghici E, Schena F, et al. Lentiviral-mediated gene therapy leads to improvement of B-cell functionality in a murine model of Wiskott-Aldrich syndrome. *J Allergy Clin Immunol* 2011; 127: 1376–1384 e1375.
46. Boztug K, Schmidt M, Schwarzer A, et al. Stem-cell gene therapy for the Wiskott-Aldrich syndrome. *N Engl J Med* 2010; 363: 1918–1927.
47. Zou J, Sweeney CL, Chou BK, et al. Oxidase-deficient neutrophils from X-linked chronic granulomatous disease iPSCs: functional correction by zinc finger nuclease-mediated safe harbor targeting. *Blood* 2011; 117: 5561–5572.
48. Suzuki N, Yamazaki S, Yamaguchi T, et al. Generation of Engraftable Haematopoietic Stem Cells From Induced Pluripotent Stem Cells by Way of Teratoma Formation. *Mol Ther* 2013; 21: 1424–1431.